TRACK CONSTRAINED PVT ESTIMATION BASED ON THE DOUBLE-DIFFERENCE TECHNIQUE FOR RAILWAY APPLICATIONS

Alessandro Neri[1], Veronica Palma[1], Francesco Rispoli[2], and Anna Maria Vegni[1]

[1] Radiolabs Consortium, Via Arrigo Cavalieri 26, Rome, Italy
Email: {*name.surname*}@radiolabs.it
[2] Ansaldo STS, S.p.A., Genoa, Italy
Email: {francesco.rispoli}@ansaldo-sts.com

ABSTRACT

In this paper we investigate the issue of positioning and tracking of a train, supported by pre-existing control and monitor system, as well as the use of satellite positioning services. The use of satellite technology can represent a viable solution to reach the goal of unmanned trains in the next future. Many forecasts consider that in a short future GNSS will meet the CENELEC railway safety standards and then will be fully operative into railway operations.
This paper presents a satellite positioning technique, which exploits the double-difference approach, in order to meet the constraint of safety level, as well as track constraint.

Index Terms— Railway applications, PVT estimation, Protection Level, Hazardous Misleading Information

1. INTRODUCTION

The range of possible Global Navigation Satellite System (GNSS) applications is diverse and largely proliferating. Early testing of extreme applications can outperform technical barriers to the general application of GNSS in various modes of safety and critical transport.
Basically, the use of GNSS in railway applications is starting to emerge. GNSS can be applied in the railway industry to significantly reduce life-cycle costs of existing signaling systems, and then allowing for new competitive safety protection where no signalization exists. As an expectation, the aim is to reach a fully automotive (*unmanned*) railway transportation system, and then to increase accuracy of existing systems.
This paper presents a Position Velocity Time (PVT) estimation technique, based on a double-differences approach, for railway applications under the rail constraint. In this scenario, we aim to evaluate the accuracy, availability, continuity, and investigate the integrity and resulting safety of GNSS on the Italian rail network.
We briefly present a Location Determination System (LDS) algorithm for determining the train location that explicitly accounts for the fact that the train location is constrained to lie on a railway track. The aim of this paper is to determine the impact of error sources on the Protection Level. While evaluations for 3D (avionics) and 2D (maritime) have been largely analyzed in the literature, the 1D case has received less attention. Thus, we provide the mathematical background for assessing the impact of various hazards on the final performance, whenever the GNSS LDS accounts for the track constraint. Nevertheless the LDS can also operate in 2D and 3D mode if needed; by fact, GNSS COTS receivers directly provide 3D estimate.
In principle, exploiting this constraint allows to estimate the train location even when only two satellites are in view. The effective reduction in the number of required satellites, to make a fix when track constraint is applied, depends on track-satellite geometry. In essence, satellites aligned along the track give more information than those at the cross-over. Satellites in excess can then be employed either to increase accuracy or to increase integrity and availability.
This paper is organized as follows. Section 2 describes recent related works on the PVT estimation analysis for railway applications. Section 3 introduces the proposed approach in case of rail constraint. In Section 4 the computation of protection level is carried out. Finally, simulation results are shown in Section 5. Conclusions are drawn at the end of the paper.

2. GNSS LDS REFERENCE ARCHITECTURE

CENELEC railways specifications impose stringent requirement on the probability of the Hazardous Misleading Information (HMI) event, defined as the probability that the magnitude of the error on the location provided by the GNSS LDS will exceed a threshold named Protection Level, conditioned to the fact that this event has not been detected, [1]-[8]. For instance, for SIL 4 compliant systems the HMI rate shall not exceed 10^{-9} during 1 hour of operation.
To meet this basic requirement the adopted architecture includes a Range and Integrity Monitoring (RIM) subsystem consisting of a set of GNSS receivers deployed along the

railway in known (geo-referenced) positions, and a central processing facility named Track Area LDS Safety (TALS) unit. TALS servers jointly analyze the measurements provided by the RIM receivers in order to detect Signal In Space (SIS) failures, as well as atmospheric anomalous behaviors. In addition, they compute the differential corrections sent to the GNSS receivers on board of the train, through the wireless link employed for the train control. In [2], the authors analyzed the case in which TALS servers were providing to the GNSS On Board Unit (OBU) corrections concerning satellite ephemerides and clock errors, as well as ionospheric and tropospheric incremental time delays.

In this paper, we adopt the Double-Difference approach for railway location computation. For sake of compactness, equations for location and protection level computation are provided for code tracking only; nevertheless, they can be extended to phase tracking in a straightforward manner.

3. TRACK CONSTRAINED DOUBLE-DIFFERENCE PVT ESTIMATE

Let $\rho_i^{Train}(k)$ and $\rho_i^{MS}(k)$ be the pseudo-ranges of the i-th satellite measured, respectively, by the OBU GNSS receiver and by the Master Station (MS). They can be expressed as:

$$\rho_i^{Train}(k) = \left\| \mathbf{X}_i^{Sat}\left[T_i^{Sat}(k)\right] - \mathbf{X}^{Train}\left[s(T_i^{Train}(k))\right] \right\| + \\ + c\Delta\tau_i^{ion,Train}(k) + c\Delta\tau_i^{trop,Train}(k) + \\ + c\delta t^{Train}(k) + n_i^{Train}(k) - c\delta t_i^{Sat}(k), \quad (1)$$

$$\rho_i^{MS}(k) = \left\| \mathbf{X}_i^{Sat}\left[T_i^{Sat}(k)\right] - \mathbf{X}^{MS} \right\| + \\ + c\Delta\tau_i^{ion,MS}(k) + c\Delta\tau_i^{trop,MS}(k) + \\ + c\delta t^{MS}(k) + n_i^{MS}(k) - c\delta t_i^{Sat}(k), \quad (2)$$

where

- $T_i^{Sat}(k)$ is the time instant on which the signal of the k-th epoch is transmitted from the i-th satellite,
- $\mathbf{X}_i^{Sat}\left[T_i^{Sat}(k)\right]$ is the coordinate vector of the i-th satellite at time $T_i^{Sat}(k)$,
- $\mathbf{X}^{MS}$ is the coordinate vector of the master station,
- $\Delta\tau_i^{ion,MS}(k)$ and $\Delta\tau_i^{ion,Train}(k)$ are the ionospheric incremental delays, along the paths from the i-th satellite to the GNSS receivers (*i.e.*, respectively, the *MS* and the OBU GNSS receiver) for the k-th epoch w.r.t. the neutral atmosphere,
- $\Delta\tau_i^{trop,MS}(k)$ and $\Delta\tau_i^{trop,Train}(k)$ are the tropospheric incremental delay, along the paths from the i-th satellite to the GNSS receivers (*i.e.*, respectively, the *MS* and the

OBU GNSS receiver) for the k-th epoch w.r.t. the neutral atmosphere,

- $\delta t_i^{Sat}(k)$ is the offset of the i-th satellite clock for the k-th epoch,
- δt^{MS} is the *MS*'s receiver clock offset,
- $n_i^{MS}(k)$ and $n_i^{Train}(k)$ are the errors of the time of arrival estimation algorithm, generated by multipath, GNSS receiver thermal noise and eventual radio frequency interference, respectively at the *MS* and the OBU GNSS receiver.

Denoting with $\mathbf{b}$ the baseline between the train receiver and the *MS*, (see [8]),

$$\mathbf{b}(k) = \mathbf{X}^{Train}\left[s(T^{Train}(k))\right] - \mathbf{X}^{MS}, \quad (3)$$

and with $\mathbf{e}_{Train}^p$ and $\mathbf{e}_{MS}^p$ the unit vectors corresponding to the lines-of-sight from the p-th satellite to the *MS*, and the OBU GNSS receiver, respectively:

$$\mathbf{e}_{MS}^p = \left[\frac{X_{p_E}^{Sat} - X_E^{MS}}{\left\| \mathbf{X}_p^{Sat} - \mathbf{X}^{MS} \right\|} \quad \frac{X_{p_N}^{Sat} - X_N^{MS}}{\left\| \mathbf{X}_p^{Sat} - \mathbf{X}^{MS} \right\|} \quad \frac{X_{p_U}^{Sat} - X_U^{MS}}{\left\| \mathbf{X}_p^{Sat} - \mathbf{X}^{MS} \right\|} \right]^T, \quad (4)$$

$$\mathbf{e}_{Train}^p = \left[\frac{X_{p_E}^{Sat} - X_E^{Train}}{\left\| \mathbf{X}_p^{Sat} - \mathbf{X}^{Train} \right\|} \quad \frac{X_{p_N}^{Sat} - X_N^{Train}}{\left\| \mathbf{X}_p^{Sat} - \mathbf{X}^{Train} \right\|} \quad \frac{X_{p_U}^{Sat} - X_U^{Train}}{\left\| \mathbf{X}_p^{Sat} - \mathbf{X}^{Train} \right\|} \right]^T \quad (5)$$

then, for the single difference SD_p between the geometric distances between the i-th satellite and the *MS* and the OBU GNSS receiver, we can write:

$$SD_p = \left\| \mathbf{X}_p^{Sat}\left[T_p^{Sat}(k)\right] - \mathbf{X}^{Train}\left[s\left(T_p^{Train}(k)\right)\right] \right\| - \\ - \left\| \mathbf{X}_p^{Sat}\left[T_p^{Sat}(k)\right] - \mathbf{X}^{MS} \right\| = \\ = r_{train}^p\left[1 - \left\langle \mathbf{e}_{train}^p, \mathbf{e}_{MS}^p \right\rangle\right] - \left\langle \mathbf{b}, \mathbf{e}_{MS}^p \right\rangle. \quad (6)$$

Without loss of the generality, assuming that the first satellite is used as pivot to compute the double-difference equations, and denoting with $DD_{p,q}$ the double difference of the single differences related to the p-th and q-th satellites, the double-difference equation can be rewritten in matrix form as follows:

$$\overline{\mathbf{DD}} = \mathbf{Hb} + \mathbf{v}, \quad (6)$$

where

$$\overline{\mathbf{DD}} = \mathbf{DD} - \Delta\mathbf{DD}, \quad (7)$$

with

$$\mathbf{DD} = \left[DD_{2,1} \quad DD_{3,1} \quad \dots \quad DD_{N_{sat},1} \right]^T, \quad (8)$$

$$\Delta\mathbf{DD} = \begin{bmatrix} r_{train}^2\left[1 - \left\langle \mathbf{e}_{train}^2, \mathbf{e}_{MS}^2 \right\rangle\right] - r_{train}^1\left[1 - \left\langle \mathbf{e}_{train}^1, \mathbf{e}_{MS}^1 \right\rangle\right] \\ r_{train}^3\left[1 - \left\langle \mathbf{e}_{train}^3, \mathbf{e}_{MS}^3 \right\rangle\right] - r_{train}^1\left[1 - \left\langle \mathbf{e}_{train}^1, \mathbf{e}_{MS}^1 \right\rangle\right] \\ \vdots \\ r_{train}^{N_{sat}}\left[1 - \left\langle \mathbf{e}_{train}^{N_{sat}}, \mathbf{e}_{MS}^{N_{sat}} \right\rangle\right] - r_{train}^1\left[1 - \left\langle \mathbf{e}_{train}^1, \mathbf{e}_{MS}^1 \right\rangle\right] \end{bmatrix}, \quad (9)$$

$$\mathbf{H} = \begin{vmatrix} e_E^1 - e_E^2 & e_N^1 - e_N^2 & e_U^1 - e_U^2 \\ e_E^1 - e_E^3 & e_N^1 - e_N^3 & e_U^1 - e_U^3 \\ \vdots & \vdots & \vdots \\ e_E^1 - e_E^{N_{sat}} & e_N^1 - e_N^{N_{sat}} & e_U^1 - e_U^{N_{sat}} \end{vmatrix}, \quad (10)$$

and the components of the equivalent receiver noise are:

$$v_{p1} = c[\Delta\tau_p^{ion,Train}(k) - \Delta\tau_p^{ion,MS}(k) - \Delta\tau_1^{ion,Train}(k) + \Delta\tau_1^{ion,MS}(k)$$

$$+ \Delta\tau_p^{trop,Train}(k) - \Delta\tau_p^{trop,MS}(k) - \Delta\tau_1^{trop,Train}(k) + \Delta\tau_1^{trop,MS}(k)] +$$

$$+ n_p^{Train}(k) - n_p^{MS}(k) - n_1^{Train}(k) - n_1^{MS}(k). \quad (11)$$

When the track constraint is imposed, the Cartesian coordinates, w.r.t. a local reference frame (*i.e.*, EST, NORTH, UP), are described as

$$\mathbf{X}^{Train}(t) = \mathbf{X}^{Train}\{s(t)\} =$$

$$= \begin{bmatrix} x_E^{Train}[s(t)] & x_N^{Train}[s(t)] & x_U^{Train}[s(t)] \end{bmatrix}^T, (13)$$

whose solution can be obtained by an iterative procedure, as described as follows. Let $\hat{s}^{(m)}$ be the train curvilinear abscissa at the *m*-th iteration, so that

$$s = \hat{s}^{(m)} + \Delta\hat{s}^{(m)}. \quad (12)$$

In addition, we pose

$$\hat{\mathbf{b}}^{(m)} = \mathbf{X}^{Train}\left[\hat{s}^{(m)}\right] - \mathbf{X}^{MS}. \quad (13)$$

Then, expanding the baseline in Taylor's series w.r.t. *s*, and with initial point $\hat{s}^{(m)}$, we have

$$\mathbf{b} \simeq \mathbf{b}^{(m)} + \left[\frac{\partial\mathbf{b}}{\partial s}\right]_{s=\hat{s}^{(m)}} \Delta s, \quad (14)$$

therefore

$$\overline{\mathbf{DD}}^{(m)} = \mathbf{H}\hat{\mathbf{b}}^{(m)} + \mathbf{H}\left[\frac{\partial\mathbf{b}}{\partial s}\right]_{s=\hat{s}^{(m)}} \Delta s + \mathbf{v}, \quad (15)$$

where

$$\overline{\mathbf{DD}}^{(m)} = \mathbf{DD} - \Delta\mathbf{DD}^{(m)}, \quad (16)$$

$$\Delta\mathbf{DD}^{(m)} = \begin{bmatrix} r_{train}^{2(m)}\left[1 - \left\langle \mathbf{e}_{train}^{2(m)}, \mathbf{e}_{MS}^2 \right\rangle\right] - r_{train}^{1(m)}\left[1 - \left\langle \mathbf{e}_{train}^{1(m)}, \mathbf{e}_{MS}^1 \right\rangle\right] \\ r_{train}^{3(m)}\left[1 - \left\langle \mathbf{e}_{train}^{3(m)}, \mathbf{e}_{MS}^3 \right\rangle\right] - r_{train}^{1(m)}\left[1 - \left\langle \mathbf{e}_{train}^{1(m)}, \mathbf{e}_{MS}^1 \right\rangle\right] \\ \vdots \\ r_{train}^{N_{sat}(m)}\left[1 - \left\langle \mathbf{e}_{train}^{N_{sat}(m)}, \mathbf{e}_{MS}^{N_{sat}} \right\rangle\right] - r_{train}^{1(m)}\left[1 - \left\langle \mathbf{e}_{train}^{1(m)}, \mathbf{e}_{MS}^1 \right\rangle\right] \end{bmatrix}, (17)$$

and

$$\mathbf{e}_{train}^{p(m)} = \frac{\mathbf{X}_p^{Sat} - \mathbf{X}^{train}[\hat{s}^{(m)}]}{\left\|\mathbf{X}_p^{Sat} - \mathbf{X}^{train}[\hat{s}^{(m)}]\right\|}, \quad r_{train}^{p(m+1)} = \left\|\mathbf{X}_p^{Sat} - \mathbf{X}^{train}[\hat{s}^{(m)}]\right\| \quad (18)$$

On the other hand,

$$\frac{\partial\mathbf{b}}{\partial s} = \frac{\partial\mathbf{X}^{Train}[s]}{\partial s} - \frac{\partial\mathbf{X}^{MS}}{\partial s} = \frac{\partial\mathbf{X}^{Train}[s]}{\partial s}, \quad (19)$$

therefore, denoting with $\mathbf{G}^{(m)}$ the following vector

$$\mathbf{G}^{(m)} = \left[\left(\frac{\partial\mathbf{X}_E^{Train}}{\partial s}\right)_{s=\hat{s}^{(m)}} \left(\frac{\partial\mathbf{X}_N^{Train}}{\partial s}\right)_{s=\hat{s}^{(m)}} \left(\frac{\partial\mathbf{X}_U^{Train}}{\partial s}\right)_{s=\hat{s}^{(m)}}\right]^T, \quad (20)$$

finally, we have

$$\mathbf{DD} - \mathbf{H}\hat{\mathbf{b}}^{(m)} = \mathbf{H}\mathbf{G}^{(m)}\Delta s + \mathbf{v}, \quad (21)$$

and the constrained estimate at the (*m*+1)-th iteration is computed as follows:

$$\hat{s}^{(m+1)} = \hat{s}^{(m)} + \mathbf{K}^{(m)}\overline{\mathbf{DD}}^{(m)}, \quad (22)$$

where the gain $\mathbf{K}^{(m)}$ is computed in accordance to the Weighted Least Square Estimation (WLSE) as

$$\mathbf{K}^{(m)} = \left(\mathbf{G}^{(m)T}\mathbf{H}^T R_{\mathbf{v}}^{-1}\mathbf{H}\mathbf{G}^{(m)}\right)^{-1}\mathbf{G}^{(m)T}\mathbf{H}^T R_{\mathbf{v}}^{-1}. \quad (23)$$

4. PROTECTION LEVEL COMPUTATION

Let us consider the event of a failure of the *p*-th satellite (or atmospheric propagation model) equivalently modeled by a satellite position error $\boldsymbol{\beta}^p$. In this case, w.r.t Figure 1, it can be easily verified that

$$\tilde{\mathbf{e}}_{train}^p = \mathbf{e}_{train}^p \frac{r_{train}^p}{\left\|r_{train}^p\mathbf{e}_{train}^p + \boldsymbol{\beta}^p\right\|} + \frac{\boldsymbol{\beta}^p}{\left\|r_{train}^p\mathbf{e}_{train}^p + \boldsymbol{\beta}^p\right\|}, \quad (24)$$

$$\tilde{\mathbf{e}}_{MS}^p = \mathbf{e}_{MS}^p \frac{r_{MS}^p}{\left\|r_{MS}^p\mathbf{e}_{MS}^p + \boldsymbol{\beta}^p\right\|} + \frac{\boldsymbol{\beta}^p}{\left\|r_{MS}^p\mathbf{e}_{MS}^p + \boldsymbol{\beta}^p\right\|}. \quad (25)$$

Thus, the single difference of the *p*-th satellite is affected by the error

$$\varepsilon_{\Delta SD}^p = \tilde{r}_{train}^p\left[\left\langle \tilde{\mathbf{e}}_{train}^p, \tilde{\mathbf{e}}_{MS}^p \right\rangle - \left\langle \mathbf{e}_{train}^p, \mathbf{e}_{MS}^p \right\rangle\right] +$$

$$+ \Delta r_{train}^p\left[1 - \left\langle \mathbf{e}_{train}^p, \mathbf{e}_{MS}^p \right\rangle\right] + \left\langle \mathbf{b}, \tilde{\mathbf{e}}_{MS}^p - \mathbf{e}_{MS}^p \right\rangle. \quad (29)$$
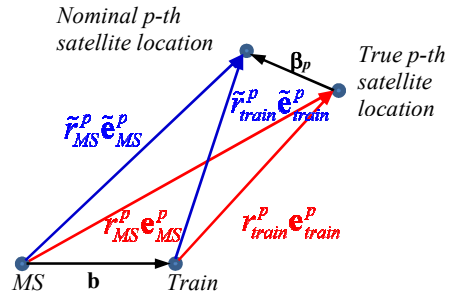
Figure 1. Faulty satellite geometry.

As a consequence, if the faulty satellite is not the pivot one (*i.e.*, in our case $p \neq 1$) the train location estimate is affected by the additional error, that is:

$$\Delta s_p^{SF}(\mathbf{\beta}^p) = \mathbf{K}_{1,p-1}\varepsilon_{\Delta SD}^p(\mathbf{\beta}^p), \quad p = 2,...,N_{sat} \qquad (26)$$

while, if the faulty satellite is the pivot one (*i.e.*, in our case *p* = 1), then we have:

$$\Delta s_1^{SF}(\mathbf{\beta}^1) = -\left[\sum_{q=1}^{N_{sat}-1} \mathbf{K}_{1,q}\right]\varepsilon_{\Delta SD}^1(\mathbf{\beta}^1) \qquad (27)$$

Denoting with $\gamma^{(i)}(\mathbf{\beta})$ the function

$$\gamma^{(i)}(\mathbf{\beta}) = \begin{cases} -\left[\sum_{q=1}^{N_{sat}-1} \mathbf{K}_{1,q}\right]\varepsilon_{\Delta SD}^i(\mathbf{\beta}) & i = 1 \\ \mathbf{K}_{1,i-1}\varepsilon_{\Delta SD}^i(\mathbf{\beta}) & i = 2,...,N_{sat} \end{cases},$$
$$(28)$$

the conditional probability that the position error magnitude will exceed the protection level, when the *i*-th satellite is faulty, becomes

$$P_{MI/MA}^{SF} = \frac{1}{2}erfc\left(\frac{PL - \gamma^{(i)}(\mathbf{\beta})}{\sqrt{2}\sigma_s}\right) + \frac{1}{2}erfc\left(\frac{PL + \gamma^{(i)}(\mathbf{\beta})}{\sqrt{2}\sigma_s}\right). \quad (29)$$

However, the computation of the HMI probability requires the evaluation of the probability that TALS will not detect the satellite fault. At this aim, let us denote with $\Delta\rho_{i,j}(k)$ the reduced pseudorange of the *i*-th satellite measured by the *j*-th RIM station. This is given by the difference between the nominal range $\hat{r}_{i,j}(k)$, based on the satellite positions computed from the data extracted from the satellite navigation message and from SBAS corrections, and the observed pseudorange $\rho_{i,j}(k)$, and also corrected by the ionospheric and tropospheric incremental delays *i.e.*, $\Delta\hat{\tau}_i^{ion}(k)$ and $\Delta\hat{\tau}_i^{trop}(k)$. This is expressed as:

$$\Delta\rho_{i,j}(k) \triangleq r_{i,j}(k) - \rho_{i,j}(k) + \Delta\tau_i^{ion}(k) + \Delta\tau_i^{trop}(k). \quad (30)$$

Let us denote with $\zeta_i(k)$ the status error of the *i*-th satellite

$$\zeta_i(k) = \begin{bmatrix} \Delta\mathbf{X}_i^{sat}(k) \\ \Delta t_i^{sat}(k) \end{bmatrix}, \qquad (31)$$

whose components are given by (*i*) the satellite position errors $\Delta\mathbf{X}_i^{sat}(k)$, equal to the difference between the actual satellite position and the position predicted on the basis of the data provided by the navigation message and SBAS data, and (*ii*) the satellite clock error $\Delta t_i^{Sat}(k)$ given by the difference between the actual clock offset and the clock offset provided by the navigation message and SBAS data, when available. Also, let $\zeta(k)$ be the vector of status errors of all N_{sat} satellites in view, and $\mathbf{z}(k)$ the vector of the satellite status errors and RIM clock offsets. It follows that the measurement equation can be written by a linearized regression model, as:

$$\Delta\tilde{\mathbf{\rho}}(k) = \mathbf{H}(k)\mathbf{z}(k) + \mathbf{v}^{RIM}(k) \qquad (32)$$

where

$$\mathbf{H}(k) = \begin{bmatrix} \mathbf{Q}^{(1)}(k) & 0 & \cdots & 0 & \mathbf{I}_{N_{RIM} \times N_{RIM}} \\ 0 & \mathbf{Q}^{(1)}(k) & \cdots & 0 & \mathbf{I}_{N_{RIM} \times N_{RIM}} \\ \vdots & \vdots & \vdots & \vdots & \vdots \\ 0 & 0 & \cdots & \mathbf{Q}^{(N_{sat})}(k) & \mathbf{I}_{N_{RIM} \times N_{RIM}} \end{bmatrix} \quad (33)$$

with

$$\mathbf{Q}^{(i)}(k) = \begin{bmatrix} \mathbf{q}_i^{(1)}(k) \\ \mathbf{q}_i^{(2)}(k) \\ \vdots \\ \mathbf{q}_i^{(N_{RIM})}(k) \end{bmatrix}, \qquad (34)$$

and $\mathbf{q}_i^{(j)}(k)$ is the vector whose first three components are the directional cosines of the vector that connects the true location of the *i*-th satellite and the *j*-th RIM, that is:

$$\mathbf{q}_i^{(j)}(k) = \begin{bmatrix} \dfrac{\partial r_{i,j}(k)}{\partial x_{i,E}^{Sat}} & \dfrac{\partial r_{i,j}(k)}{\partial x_{i,N}^{Sat}} & \dfrac{\partial r_{i,j}(k)}{\partial x_{i,U}^{Sat}} & -1 \end{bmatrix}$$
$$= \begin{bmatrix} \dfrac{x_{i,1}^{Sat} - x_{j,1}^{RIM}}{\|\mathbf{X}_i^{Sat} - \mathbf{X}_j^{RIM}\|} & \dfrac{x_{i,2}^{Sat} - x_{j,2}^{RIM}}{\|\mathbf{X}_i^{Sat} - \mathbf{X}_j^{RIM}\|} & \dfrac{x_{i,3}^{Sat} - x_{j,3}^{RIM}}{\|\mathbf{X}_i^{Sat} - \mathbf{X}_j^{RIM}\|} & -1 \end{bmatrix}, \quad (41)$$

Finally, $\mathbf{v}^{RIM}(k)$ is modeled as a Gaussian *m*-variate random variable with expectation $\mathbf{\mu}$ and covariance matrix $\mathbf{R_v}$. Satellite status errors and RIM clock offsets can then be estimated by means of WLSE or MMSE algorithms. Let us assume here, without loss of generality that WLSE is adopted, then for the estimate of $\mathbf{z}(k)$ we have

$$\hat{\mathbf{z}}(k) = \mathbf{\Gamma}\Delta\tilde{\mathbf{\rho}}(k), \qquad (35)$$

where

$$\mathbf{\Gamma} = \left(\mathbf{H}^T R_v^{-1}\mathbf{H}\right)^{-1}\mathbf{H}^T R_v^{-1}. \qquad (36)$$

Then, for each visible satellite the integrity algorithm monitors the behavior of the least square residuals $\hat{\mathbf{v}}^{(i)}$ of the reduced pseudoranges, that is

$$\hat{\mathbf{v}}_i = \Delta\mathbf{\rho}_i - \mathbf{Q}^{(i)}\hat{\zeta}_i - c\delta\hat{\mathbf{t}}^{RIM}. \qquad (37)$$

More specifically, the square of L^2 weighted norm

$$\xi_i^2 = \left(\hat{\mathbf{v}}^{(i)}\right)^T \mathbf{R}_{\hat{\mathbf{v}}^{(i)}}^{-1}\hat{\mathbf{v}}^{(i)}, \qquad (38)$$

with

$$\mathbf{R}_{\hat{\mathbf{v}}} = [\mathbf{I} - \mathbf{\Gamma C}]\mathbf{R_v}[\mathbf{I} - \mathbf{\Gamma C}] \qquad (39)$$

is compared to a threshold *T*. If ξ^2 exceeds the threshold the satellite is marked as faulty and it is excluded from on board fix computation. The threshold is set in accordance to a given false alarm probability P_{fa}.

4. EXPERIMENTAL RESULTS

The proposed algorithm has been assessed by post-processing in Matlab environment a set of raw data collected with COTS receivers. The set of real data has been acquired during a measurement campaign along the GRA Annular Ring highway of Rome.

Two RIMs have been displaced along the highway, acting as masters, and equipped with two different receivers (*i.e.*, NVS and u-blox). A car also equipped with both types of receivers has been used as rover. The path of the car from the position of RIM 1 up to position of RIM 2 is shown in Figure 2 (blue and red lines). Both the receivers of the RIMs have been used for PVT estimation, in several combinations. For sake of space only a couple of test results are reported here. Figure 3 and Figure 4 show the positioning errors versus the ground truth for the cases of RIM 1, and RIM 2 acting as masters, respectively. More in detail, in Figure 3 (case 1) the NVS receiver of RIM 1, and the u-blox receiver for the rover have been used; in Figure 4 (case 2) the u-blox receivers for both RIM 2 and rover have been employed. We observe that for case 1 the error is mainly bounded in the range [-4, +4] m, while in case 2, the positioning error is mostly limited in [-4, +2] m. This is essentially due to the better performance of the u-blox receiver w.r.t. the NVS one. Notice that in both the cases, we can observe a few measurements outside theses ranges; this is due to multipath effect, experienced at the entrance and exit from the tunnels, encountered along the GRA.

5. CONCLUSIONS

In this paper, a novel double difference algorithm for train location determination that explicitly accounts for the track constraint has been proposed. Real time algorithms also include evaluation of the achievable Protection Level, as a function of satellite geometry and computation of the HMIR.

6. REFERENCES

[1] A. Filip, J. Beugin, and J. Marais, "Safety Concept of Railway Signalling Based on Galileo Safety-of-Life Service," COMPRAIL, Toledo, Spain, Sept. 15-17, 2008, pp. 103-112.

[2] A. Neri, A. Filip, F. Rispoli, and A.M. Vegni, "An Analytical Evaluation for Hazardous Failure Rate in a Satellite-based Train Positioning System with reference to the ERTMS Train Control Systems", ION 2012, Nashville, 2012.

[3] A. Filip, "Dependability Assessment of Satellite Based Augmentation System for Signalling and Train Control," Intl. Heavy Haul Association Conference (IHHA 2011), Calgary, Canada, Jun. 19-22, 2011.

[4] A. Filip, "Safety Aspects of GNSS Based Train Position Determination for Railway Signalling," UIC Galileo for Rail Symposium, Paris, Oct. 18-19, 2007.

[5] A. Filip, J. Beugin, J. Marais, and H. Mocek, "A relation among GNSS quality measures and railway RAMS attributes," CERGAL '2008, Braunschweig, Germany, Apr. 2-3, 2008.

[6] Galileo Integrity Concept, ESA document ESA-DEUI-NG-TN/01331, 2005.

[7] S. Pullen, T., Walter, and P. Enge, "SBAS and GBAS Integrity for Non-Aviation Users: Moving Away from Specific Risk," Intl. Tech. Meeting of the Institute of Navigation, San Diego, CA, USA, pp.533-543, 2011.

Figure 2. (*Blue and red lines*) Ground truth of GRA highway in Rome (Italy). The *blue* (red) *line* is the portion of the track (not) taken into account in our simulations.

Figure 3. Positioning errors vs. ground truth (case 1).

Figure 4. Positioning errors vs. ground truth (case 2).

[8] A. Filip, H. Mocek, and J. Suchánek, "Significance of the Galileo Signal-in-Space Integrity and Continuity for Railway Signalling and Train Control," 8th World Congress on Railway Research (WCRR), Seoul, Korea, 2008.

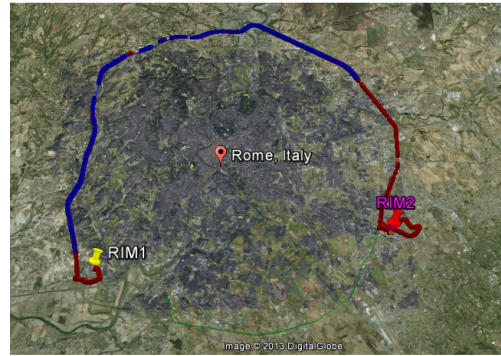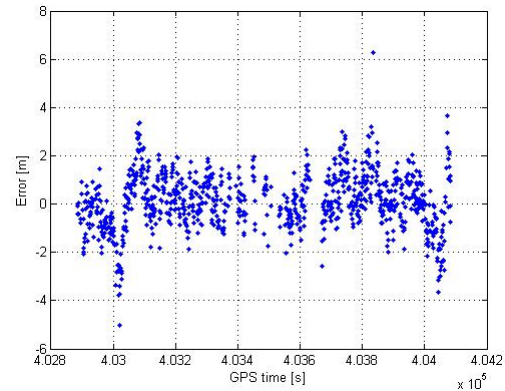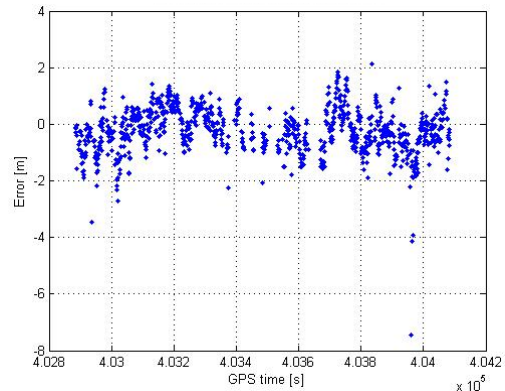[9] E.D. Kaplan, and C.J. Hegarty, *Understanding the GPS*, GeoResearch, Inc., pp. 407, 1996.